Available online at www.sciencedirect.com
SCIENCE DIRECT
Dyes and Pigments 68 (2006) 217–226
DYES and PIGMENTS
www.elsevier.com/locate/dyepig

Optical properties and aggregation of novel azo-dyes bearing an end-capped oligo(ethylene glycol) side chain in solution, solid state and Langmuir–Blodgett films

Ernesto Rivera [a,*], María del Pilar Carreón-Castro [b], Ignacio Buendía [a], Gerardo Cedillo [a]

[a] *Instituto de Investigaciones en Materiales UNAM, Circuito Exterior Ciudad Universitaria C.P. 04510, México D.F. México*
[b] *Instituto de Ciencias Nucleares UNAM, Circuito Exterior Ciudad Universitaria C.P. 04510, México D.F. México*

Received 28 August 2004; received in revised form 25 January 2005; accepted 2 February 2005
Available online 9 April 2005

Abstract

Optical properties and aggregation of two novel azo-dyes *N*-methyl-*N*-{4-[(*E*)-(4-nitrophenyl)diazenyl]phenyl}-*N*-(3,6,9-trioxadecas-1-yl)amine (**RED-PEGM-3**) and *N*-methyl-*N*-{4-[(*E*)-(4-nitrophenyl)diazenyl] phenyl}-*N*-(3,6,9,12,15,18,21,24-octaoxapentaeicos-1-yl)amine (**RED-PEGM-8**) were studied by UV–vis spectroscopy in solution, solid state and Langmuir–Blodgett films. The results were compared to those obtained for their precursor 1-amino-4′-nitroazobenzene (Disperse Orange 3, **DO3**) and 1-*N*-methylamino-4′-nitroazobenzene (**RED-H**). Increasing the polarity of methanol:water mixtures gave rise to the formation of H-aggregates for all dyes. Similar aggregates were also detected in cast films. NOESY, 2D ^{1}H NMR experiments carried out in aqueous solutions of **RED-PEGM-8** revealed the formation of atypical antiparallel H-aggregates. Only **RED-PEGM-3** gave traces of J-aggregates in the solid state. **RED-PEGM-3** and **RED-PEGM-8** readily form J-aggregates in Y-type Langmuir–Blodgett films.

Keywords: Aggregation; Azobenzene; Poly(ethylene glycol); UV–vis spectroscopy; LB films

1. Introduction

Azobenzenes, which were first used as color dyes, have been widely studied by many research groups. Rau classified azobenzenes into three main groups based on their photochemical behavior [1]. Unsubstituted azobenzene belongs to the first group which is simply called ‘‘azobenzene’’ and is considered to be a photochromic molecule because it has two possible isomers which each exhibit two bands due to $\pi-\pi^*$ and $n-\pi^*$ transitions [2]. The *trans*, $\pi-\pi^*$ band is typically more intense than the *cis*, $n-\pi^*$ transition and the two transitions tend to overlap poorly. The second group is called ‘‘amino-azobenzene’’ and the azos in this class exhibit significant overlap of the $\pi-\pi^*$ and $n-\pi^*$ bands. Finally, substituted azobenzenes bearing electron-donor and electron-acceptor groups belong to the third classification known as ‘‘pseudostilbene’’ where the $\pi-\pi^*$ and $n-\pi^*$ bands are inverted on the energy scale (relative to the azobenzene class) and become practically superimposed [1].

Chemical or physical incorporation of pseudostilbene-class azobenzenes into a polymer provides the formation of very versatile materials from an applications point of

* Corresponding author. Fax: +52 55 56 16 12 01.
E-mail address: riverage@zinalco.iimatercu.unam.mx (E. Rivera).

0143-7208/$ - see front matter © 2005 Elsevier Ltd. All rights reserved.
doi:10.1016/j.dyepig.2005.02.001

view. Upon illumination with absorbing radiation, the stable *trans*-chromophore is converted to the *cis*-isomer, which rapidly reverts back to the *trans*-state causing physical displacement of the molecule. Irradiation from a linearly polarized beam induces *trans–cis–trans* isomerization cycles only along the chromophore polarization axis, thus causing physical displacement of the molecular long axis until the polarization axis is perpendicular to the beam's polarization. In other words, any azobenzene group which lie perpendicular to the light polarization will not photoisomerize. The azo-groups that do isomerize will continue moving slightly in the process, and if at the end of a photoisomerization cycle they fall perpendicular to the light polarization, they will become inert to light [3]. Amino–nitro substituted azobenzenes have also been widely studied for this purpose. This research field has grown significantly and there are several reviews covering the topic of azobenzene photoisomerization in polymer structures [4–8]. Certain polymers bearing amino–nitro substituted azobenzenes, such as those studied by Natansohn et al. exhibit very interesting opto-electronic applications [9–11]. In general, these polymers, as other amino–nitro substituted azobenzene dyes, exhibit a maximum absorption wavelength in the 440–500 nm region.

On the other hand, aggregation has been studied for several azobenzene dyes in various environments. There are mainly three types of aggregates: H-aggregates where chromophores are paired in a face to face way, J-aggregates where the molecules are coupled in a head to tail or head to head way, and oblique aggregates [12]. In these materials, both J- and H-type aggregates have been observed [13–15]. Polymers of the pXMAN series, whose synthesis and structure have been previously reported in the literature [16], tend to form both H- and J-aggregates depending on their structure and environment. For instance, p4MAN exhibited H-aggregation in the solid state ($\lambda_{agg} = 402$ nm, $\lambda_{max} = 446$ nm). In these aggregates, azobenzene groups are coupled in an antiparallel way giving rise to stable orange films [17]. Aggregation can be broken-up through *trans–cis–trans* photoisomerization by irradiating with polarized light to give red films, where azobenzenes are randomly oriented. This photochromic phenomenon has been used for microlithography and optical storage [2,18].

Previously, we reported the synthesis and characterization of amphiphilic azobenzene dyes bearing an end-capped poly(ethylene glycol) side chain (**PEGM**): *N*-methyl-*N*-{4-[(*E*)-(4-nitrophenyl)diazenyl]phenyl}-*N*-(3,6,9,12,15,18,21,24-octaoxapentaeicos-1-yl)amine (**RED-PEGM-8**) [19]. In this work, we studied the aggregation of the dye and its homologue *N*-methyl-*N*-{4-[(*E*)-(4-nitrophenyl)diazenyl] phenyl}-*N*-(3,6,9-trioxadecas-1-yl) amine (**RED-PEGM-3**) in various environments. Aggregation of other related dyes such as 1-*N*-methylamino-4′-nitroazobenzene (**RED-H**) and 1-amino-4′-nitroazobenzene (Disperse Orange 3, **DO3**) were also studied for comparison. In summary, we study the optical properties and aggregation exhibited by a series of azobenzene dyes in solution, solid state and LB films by UV–vis and in some cases by ^{1}H NMR spectroscopy. The effect of the PEGM chain length on the material's optical properties and aggregation properties is discussed.

2. Experimental section

1-*N*-Methylamino-4′-nitroazobenzene (**RED-H**) and 1-*N*,*N*-dimethylamino-4′-nitroazobenzene (**RED-Me**) were prepared according to the procedures published in the literature for similar compounds [16]. The syntheses of *N*-methyl-*N*-{4-[(*E*)-(4-nitrophenyl)diazenyl]phenyl}-*N*-(3,6,9-trioxadecas-1-yl)amine (**RED-PEGM-3**) and *N*-methyl-*N*-{4-[(*E*)-(4-nitrophenyl) diazenyl]phenyl}-*N*-(3,6,9,12,15,18,21,24-octaoxapentacos-1-yl)amine (**RED-PEGM-8**) was carried out according to the method previously reported [19]. 1-Amino-4′-nitroazobenzene or Disperse Orange 3 (**DO3**) was purchased from Aldrich and purified by crystallization from ethanol prior to use.

All dyes were dissolved in spectral quality solvents purchased from Aldrich. Absorption spectra were recorded on a Varian Cary 1 Bio UV–vis (model 8452A) spectrophotometer at room temperature using 1 cm quartz cells. The ^{1}H NMR spectra in solution were recorded at room temperature on a Bruker Avance 400 spectrometer. Dipole moments (μ) of the dyes were estimated by AM1 and PM3 semi-empirical methods and by DFT calculations using B3LYP/cc-pVTZ(-f)+//B3LYP/G-31/g* method [20].

Langmuir–Blodgett membranes were prepared using an LB trough NIMA 622D2 (NIMA Technology Coventry, UK) equipped with a Wilhelmy plate surface pressure sensor. Spreading solutions were prepared by dissolving the dyes in chloroform (HPLC grade) in order to obtain concentrations in the range of 0.8–1.5 mg/ml. A monolayer was formed by spreading 100–150 μl of the solution on water subphase, which had been purified by a Milli-Q system (Millipore), $\rho =$ 18.2 MΩ cm. Films were compressed after 15–20 min of equilibration with a constant barrier speed of 5 cm^2/min. Isotherms were recorded at 22 ± 1 °C. Multilayers were formed by depositing monolayers at a target pressure of 25 mN/m and with a dipper speed of 5–10 mm/min and a transfer ratio of about 0.8–1.0 was observed. Quartz was used as a substrate in this work and the quartz panes were washed with chloroform, acetone and ethanol successively. The cleaning process was performed in an ultrasonic bath. Clean substrates (quartz and glass) were hydrophobized by treating them with

ferric stearate prior to deposition. Y-type LB multilayers were prepared with **RED-PEGM-3** and **RED-PEGM-8**.

3. Results and discussion

In the present work, we study the optical properties and aggregation of *N*-methyl-*N*-{4-[(*E*)-(4-nitrophenyl)-diazenyl]phenyl}-*N*-(3,6,9-trioxadecas-1-yl)amine (**RED-PEGM-3**), *N*-methyl-*N*-{4-[(*E*)-(4-nitrophenyl) diazenyl] phenyl}-*N*-(3,6,9,12,15,18,21,24-octaoxapentaeicos-1-yl) amine (**RED-PEGM-8**) in solution and in the solid state. The results were compared with those obtained for their non-amphiphilic precursors 1-amino-4′-nitroazobenzene (Disperse Orange 3, **DO3**), 1-*N*,*N*-dimethylamino-4′-nitroazobenzene (**RED-Me**) and 1-*N*-methylamino-4′-nitroazobenzene (**RED-H**). Moreover, aggregation of the **RED-PEGM** dyes was also studied in Y-type LB films. The structures of these azo-dyes are shown in Fig. 1.

Azobenzene is characterized spectroscopically by a low-intensity $n \rightarrow \pi^*$ band in the visible region of the spectrum and a high-intensity $\pi \rightarrow \pi^*$ band in the UV. Substitution by an electron-donor and an electron-withdrawing group in different rings of the azobenzene unit, like in 4-dimethylamino-4′-nitro-azobenzene, increases the dipole moment and consequently the charge transfer character (CT) of the $\pi \rightarrow \pi^*$ transition along the molecular long axis and gives rise to a red-shift of the corresponding band, which overlaps with the weak $n \rightarrow \pi^*$ band [1]. The CT character of this band causes a strong dependence of the band position on the solvent polarity [21].

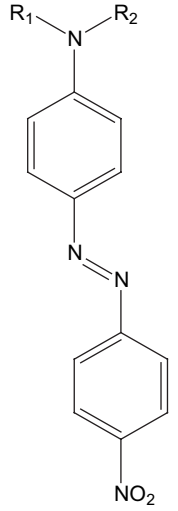

DO3 : $R_1 = R_2 = H$
RED-H : $R_1 = CH_3$, $R_2 = H$
RED-Me : $R_1 = R_2 = CH_3$
RED-PEGM-3 : $R_1 = CH_3$, $R_2 = (CH_2CH_2O)_3CH_3$
RED-PEGM-8 : $R_1 = CH_3$, $R_2 = (CH_2CH_2O)_8CH_3$

Fig. 1. Structures of the azo-compounds.

Dipole moments of the dyes were estimated by semi-empirical calculations using AM1 and PM3 methods and further by DFT calculations. The results are summarized in Table 1. AM1 semi-empirical calculations provided a good approximation of the dipole moment values (μ) for the precursor dyes, showing a decreasing polarity of the dyes as follows: **RED-Me** > **RED-H** > **DO3**. However, PM3 gave a very low μ value for **RED-H** (7.6 D) which is expected to be more polar than **DO3** according to its structure. Both AM1 and PM3 methods predicted a higher μ value for **RED-PEGM-3** than for its homologue **RED-PEGM-8**. Longer end-capped poly(ethylene glycol) side chains result in an overall decreased polarity effect on the dye. This is due to the high electron-withdrawing inductive effect, which exists along the σ bonds, due to the oxygen atoms present in the PEGM segment. Unfortunately, semi-empirical methods provide no good correlation between the μ values obtained for the dye series. For this reason, we performed DFT calculations in order to get more realistic values. DFT methods take into account electronic correlation which in combination with large basis set allows one to obtain correct electron-density distribution in the molecule. According to this method, the polarity of the dyes, in decreasing order is as follows: **RED-Me** > **RED-H** > **RED-PEGM-3** > **DO3** > **RED-PEGM-8**, which is reasonable taking into account the structure of the different azobenzenes. Methyl groups bound to the amino group significantly enhance the inductive electron-donor effect in the molecule; making **RED-Me** more polar than **RED-H** and making **RED-H** more polar than **DO3**. On the other hand, **RED-PEGM-3** possesses an intermediate μ value between those of **RED-H** and **DO3**. This is due to the electron-withdrawing inductive effect of the oxygen atoms, which decreases the electron-donor character of the amino group in this molecule. All the three methods predicted the lowest μ value for **RED-PEGM-8**, which can be explained by the higher inductive electron-withdrawing effect of the longer PEGM chain. Optical properties of all dyes were studied by absorption spectroscopy in various environments and the results are summarized in Table 2.

Table 1
Dipole moments of the azo-dyes calculated by semi-empirical and DFT methods

Azo-dye	AM1 (D)	PM3 (D)	DFT[a] (D)
DO3	9.11	8.88	9.92
RED-H	9.27	7.61	11.1
RED-Me	9.40	9.02	11.6
RED-PEGM-3	10.3	8.15	10.4
RED-PEGM-8	7.42	7.59	7.98

[a] Using B3LYP/cc-pVTZ(-f)+//B3LYP/G-31g* method.

Table 2
Absorption wavelength for the different dyes

System	**DO3** (nm)	**RED-H** (nm)	**RED-Me** (nm)	**RED-PEGM-3** (nm)	**RED-PEGM-8** (nm)
Methanol	438	464	472	478	480
Methanol:H_2O 80:20	438	476	488	488	490
Methanol:H_2O 60:40	438	421[a]	492	492	492
		480			
Methanol:H_2O 40:60	438	418[a]	–	498	498
		484			
Methanol:H_2O 20:80	404[a]	414[a]	–	402[a]	500
	438	488		500	
H_2O	–	–	–	–	402[a]
					500
Casted film ($CHCl_3$)	402–403	402[a]	–	407[a]	404[a]
		500		490	492
				500[b]	508[b]
LB film (10 layers)	–	–	–	473	490
(40 layers)				486	515

[a] Band due to the H-aggregates.
[b] Shoulder due to the J-aggregates.

3.1. Aggregation of the azo-dyes in solution

UV–vis spectra of **RED-PEGM-3** exhibit a maximum absorption band at $\lambda_{max} = 477$ nm in both $CHCl_3$ and THF, and a maximum absorption of $\lambda_{max} = 478$ nm in methanol. No aggregation was observed in these solvents, even at elevated dye concentrations. Increasing the polarity of methanol–water solvent mixtures gave rise to a λ_{max} red-shift, due to the increased CT character of molecule. No significant aggregation for this dye in mixtures of methanol–water: 80:20, 60:40 and 40:60, was detected. However, a methanol–water mixture of 20:80 **RED-PEGM-3** shows a maximum absorption band at $\lambda_{max} = 494$ nm (Fig. 2) and subsequent increase of the dye concentration leads to the appearance of an additional band in the blue region at $\lambda = 402$ nm. This less intense blue-shifted band results from the formation of H-aggregates, and no further changes where observed in the red-shifted region of the spectrum suggesting a lack of J-aggregates.

^{1}H NMR, 2D NOESY experiments confirmed that **RED-PEGM-3**, like other azobenzene dyes, undergo aggregation in a typical parallel way, as has already been stated in the literature [12]. Also, ^{1}H NMR, 2D NOESY of **RED-PEGM-3** in CD_3OD:D_2O (20:80) at elevated concentration (Fig. 3) only shows interactions of the aromatic protons with themselves and weak intermolecular interactions between H^1 and H^2 (see Scheme 1). Indeed, when **RED-PEGM-3** forms H-aggregates, molecules are paired in a parallel way "face to face". It is very well known that this arrangement is favored according to Davidov's theory [12].

On the other hand, **RED-PEGM-8** exhibits maximum absorption bands at $\lambda_{max} = 477$ nm in $CHCl_3$, $\lambda_{max} = 479$ nm in THF and $\lambda_{max} = 480$ nm in methanol. No aggregates were detected in either the concentrated or dilute solutions of these solvents or in methanol–water mixtures. The long PEGM segment of the molecule is responsible for this behavior because it confers water solubility to the dye. The absorption spectrum of **RED-PEGM-8** in diluted aqueous solution exhibits a maximum absorption at $\lambda_{max} = 500$ nm (Fig. 4) but an additional band at $\lambda = 402$ nm does originate upon increasing the dye concentration, which reveals the formation of H-aggregates.

Aggregation of **RED-PEGM-8** can be also monitored by ^{1}H NMR spectroscopy, which is more sensitive than absorption spectroscopy. The ^{1}H NMR spectral

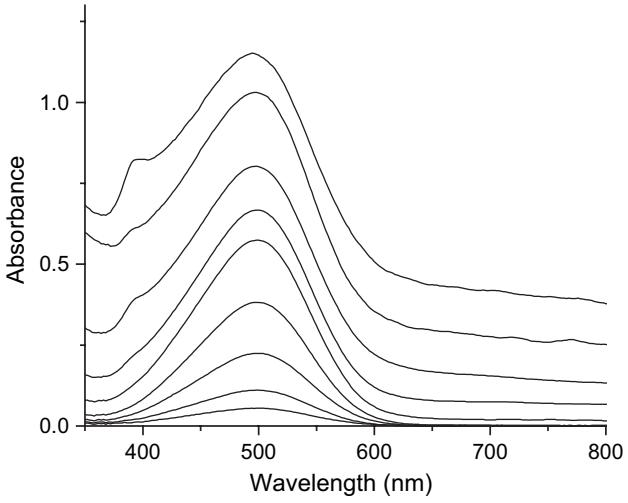

Fig. 2. UV–vis spectra of **RED-PEGM-3** in methanol:water 20:80 at different concentrations: from the top to the bottom: (a) 0.0005 M, (b) 2.5×10^{-4} M, (c) 1.87×10^{-4} M, (d) 1.25×10^{-4} M, (e) 7.5×10^{-5} M, (f) 3.75×10^{-5} M, (g) 1.82×10^{-5} M, (h) 0.93×10^{-5} M, (i) 0.46×10^{-5} M.

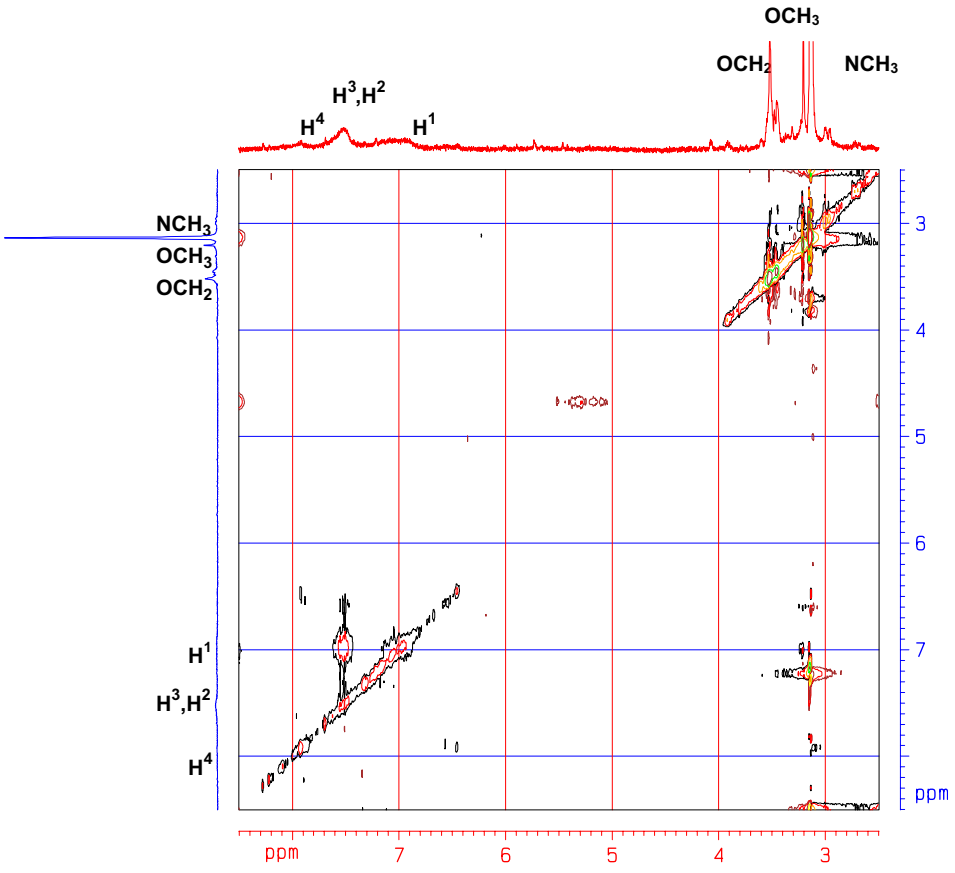

Fig. 3. ^{1}H NMR, 2D NOESY of **RED-PEGM-3** (0.0005 M) in CD_3OD:D_2O 20:80.

aromatic region of **RED-PEGM-8** in different media is shown in Fig. 5. Although no aggregation of **RED-PEGM-8** is observed in methanol or methanol–water mixtures by UV–vis methods, aromatic ^{1}H NMR signals observed for methanol:water mixtures with ratios above 40:60 exhibit large broadening and an up-field shift as compared to the results obtained in $CDCl_3$ [19]. This suggests an increased molecular electron density because of intermolecular π–π bonding interactions (H-aggregation). The ^{1}H NMR spectrum of **RED-PEGM-8** in CD_3OD solution (Fig. 5, see Scheme 1) shows four well-defined signals at $\delta = 8.35$ (d, $J = 9.2$ Hz ,H^4), 7.94 (d, $J = 8.8$ Hz, H^2), 7.87 (d, $J = 9.2$ Hz, H^3), and 6.89 (d, $J = 9.2$ Hz, H^1) ppm belonging to aromatic protons. By contrast, these signals are remarkably broader in D_2O and appear at $\delta = 7.11$ (H^4), 6.69 (protons H^2 and H^3) and 6.0 (H^1) ppm, an up-field shift of 1.21 ppm when compared to the results obtained when employing CD_3OD as a solvent. This behavior indicates the existence of strong intermolecular interactions (aggregation) in D_2O, as was previously detected by absorption spectroscopy (Fig. 4). According to ^{1}H NMR experiments, molecular association begins to occur even at lower water content concentrations, such as CD_3OD:D_2O 40:60, even though UV–vis spectroscopy only detected aggregation at higher water content concentrations.

^{1}H NMR, 2D NOESY data of **RED-PEGM-8** carried out in D_2O solution (Fig. 6) under conditions favoring H-aggregation, showed that molecules are associated in

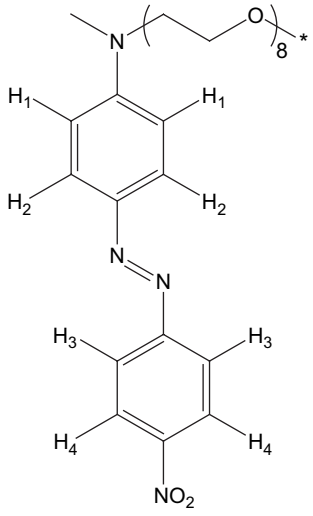

Scheme 1.

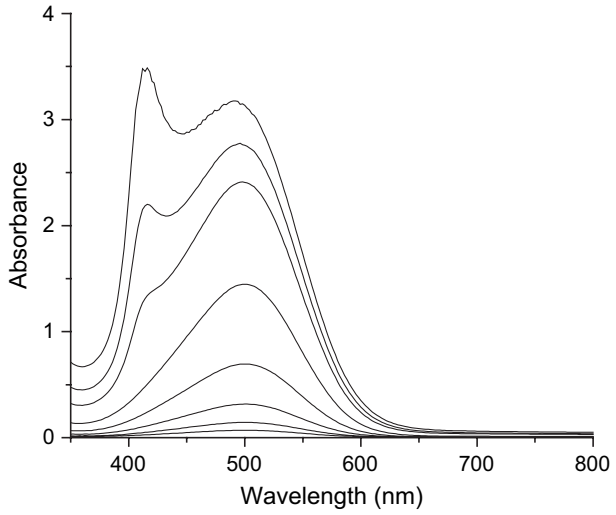

Fig. 4. UV–vis spectra of **RED-PEGM-8** in water 100% at different concentrations: from the top to the bottom: (a) 0.0005 M, (b) 2.5×10^{-4} M, (c) 1.87×10^{-4} M, (d) 1.25×10^{-4} M, (e) 7.5×10^{-5} M, (f) 3.75×10^{-5} M, (g) 1.82×10^{-5} M, (h) 0.93×10^{-5} M, (i) 0.46×10^{-5} M.

an atypical antiparallel fashion. As we can see, in the ^{1}H NMR, 2D NOESY spectrum of this dye, H^4 interacts with H^2 and the protons of N–CH_3 interact with H^3 and H^4 (see Scheme 1). These interactions can only occur in an intermolecular fashion and suggest that the molecules aggregate such that the amino group of one molecule faces the nitro group of the other. Therefore, molecules are paired in an antiparallel way with partial overlap of the azobenzene chromophores. This can be explained by enhanced steric effects, due to the eight units of ethylene glycol in the PEGM segment making the molecule rather bulky. A similar behavior was reported for azo-polymers of the pXMAN series in spin-cast films [17]. Antiparallel association is uncommon for the majority of aromatic compounds according to Davidov's theory [12].

Another interesting fact is that the ^{1}H NMR, 2D NOESY spectrum of **RED-PEGM-8** shows significant interaction of the OCH_2 protons of the PEGM chain with protons H^2, H^3 and H^4. This shows evidence of the formation of an intramolecular CT complex in aqueous solutions due to the coiling of the long PEGM segment

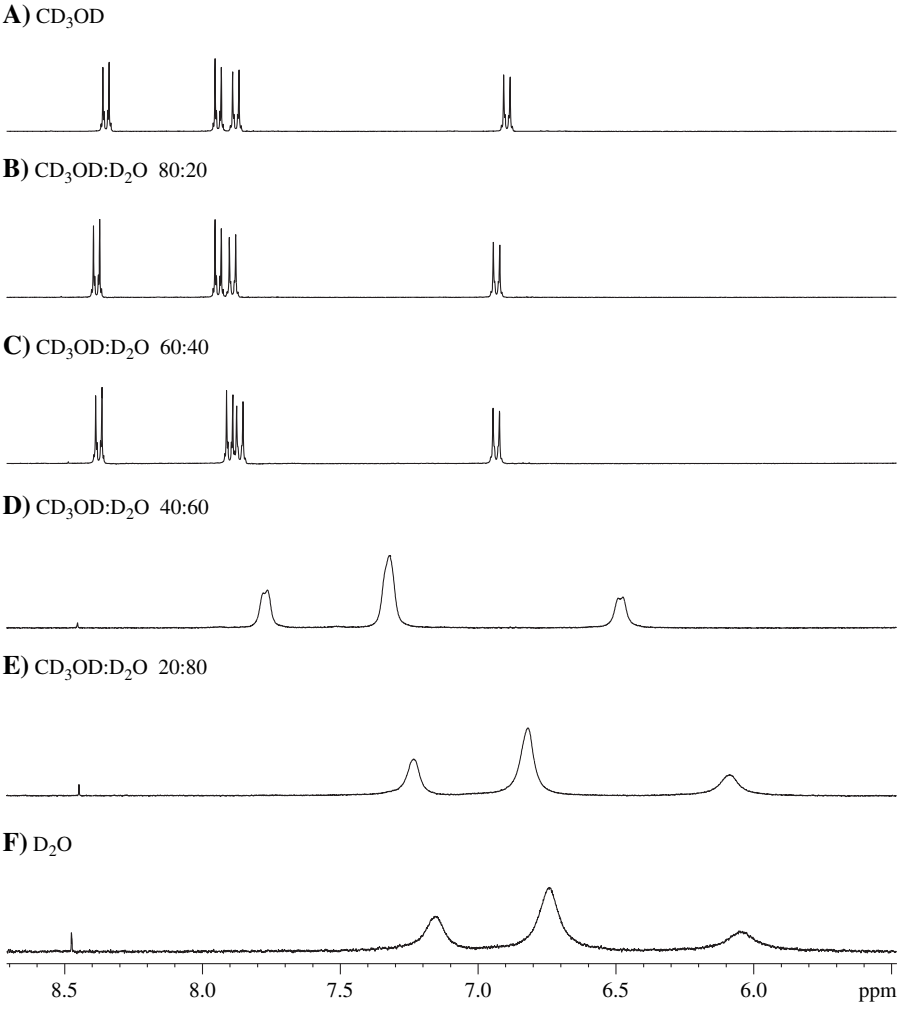

Fig. 5. ^{1}H NMR of **RED-PEGM-8** (0.0005 M) in different methanol:water systems.

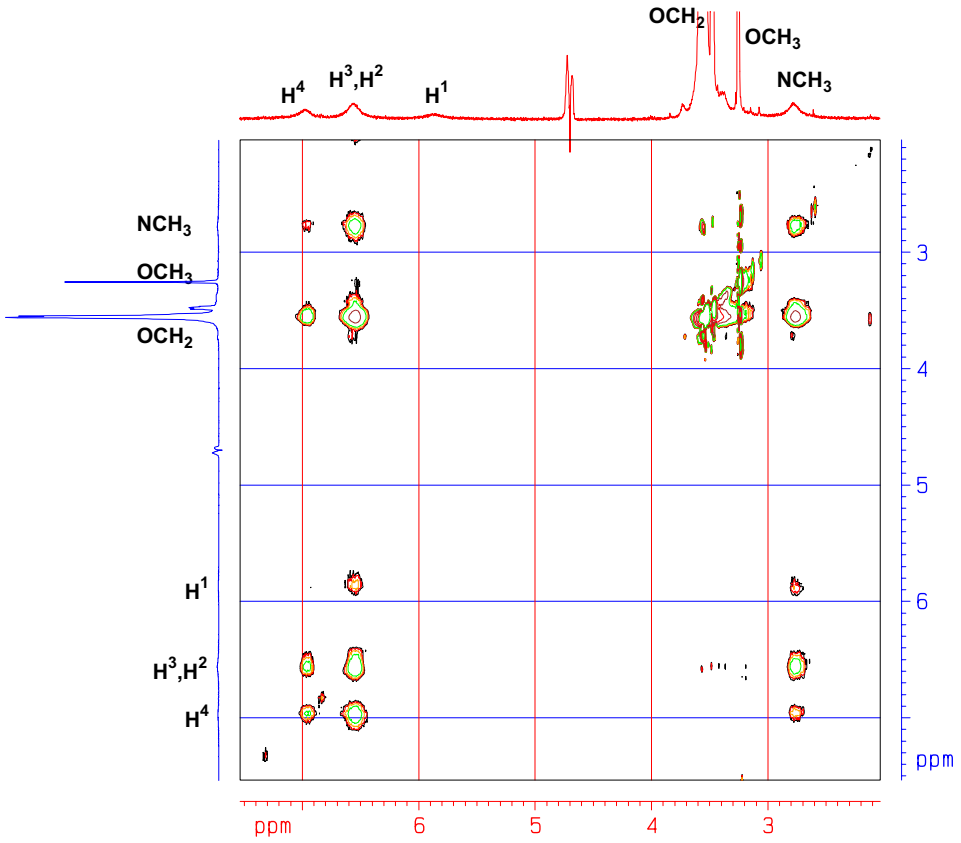

Fig. 6. ^{1}H NMR, 2D NOESY of **RED-PEGM-8** (0.0005 M) in D_2O.

around the azobenzene unit. In **RED-PEGM-8**, the poly(ethylene glycol) segment is long enough to surround the aromatic group, thereby stabilizing the electron-withdrawing nitro group with the electron rich oxygen atoms of the PEGM chain. In addition, the hydrophilic PEGM segment likely protects the hydrophobic azobenzene group from the aqueous medium. Two **RED-PEGM-8** molecules in the associated state forming an H-aggregate are represented in Fig. 7. Unlike **RED-PEGM-8**, the shorter PEGM chain of **RED-PEGM-3** is not able to surround the aromatic part of the molecule to form such kinds of complexes.

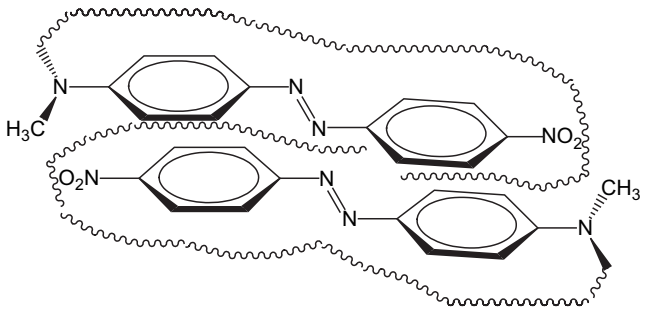

Fig. 7. Structure of **RED-PEGM-8** H-aggregates in aqueous solution.

Aggregation of the non-amphiphilic precursor dyes **DO3**, **RED-H** and **RED-Me** was also studied. Absorption spectra of **DO3** and **RED-H** recorded in 100% methanol at different concentrations exhibit a maximum absorption at about $\lambda_{max} = 438$ nm without aggregation. Relatively dilute solutions of **DO3** in mixtures of methanol:water behaved similarly. However, elevated concentrations of **DO3** in methanol:water 20:80 solutions exhibited a discrete shoulder which appears at $\lambda = 404$ nm, as shown in Fig. 8 (normalized spectra). The different spectral characteristics observed for high and low concentrations of **DO3** in methanol:water 20:80 solutions, suggest that only the highly concentrated samples contain H-aggregates.

On the other hand, **RED-H** exhibited a maximum absorption wavelength at $\lambda_{max} = 464$ nm in dilute methanol solutions and increasing the polarity of the solvent shifted this band to longer wavelengths. Increasing concentration of this dye in methanol:water 60:40, 40:60 (Fig. 9), 20:80 solutions, showed the formation of H-aggregates by the appearance of an additional band in the blue region between 414 and 421 nm and it was found that more polar environments resulted in more intense aggregation bands.

Our attempts to monitor aggregation in **RED-Me** solutions failed due to solubility limitations. In methanol,

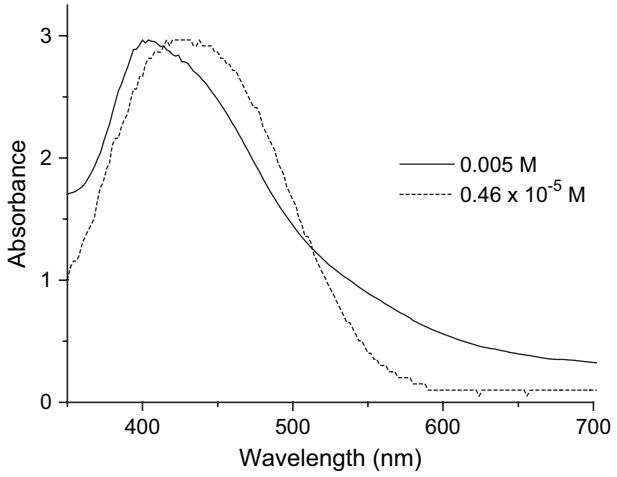

Fig. 8. Normalized UV–vis spectra of **DO3** in methanol:water 20:80. (a) 0.0005 M, (b) 0.46×10^{-5} M.

methanol:water 80:20 and 60:40 solutions, this compound shows maximum absorption at $\lambda_{max} = 472$ nm without aggregation. However, in methanol: water 40:60 the solution becomes opaque and increasing the dye concentration results in phase separation.

3.2. Aggregation of the azo-dyes in the solid state (casted films)

Films of all these dyes were prepared by casting from $CHCl_3$ solutions. The absorption spectra of **RED-PEGM-3**, **RED-PEGM-8** and **RED-H** in casted films are shown in Fig. 10. The UV–vis spectrum of **RED-PEGM-3** in the solid state exhibits maximum absorption at $\lambda_{max} = 490$ nm (12 nm red-shifted compared to methanol solution) preceded by a band in the blue region at $\lambda = 407$ nm arising from H-aggregates. It is worthwhile to point out that a third band is visible at about $\lambda = 500$ nm overlapping with the maximum absorption band (Fig. 10); this can be attributed to the presence of J-aggregate traces in solid state.

On the other hand, **RED-PEGM-8** shows maximum absorption at $\lambda_{max} = 492$ nm in the film (12 nm red-shifted compared with methanol solution) preceded by a band at $\lambda = 404$ nm, due to H-aggregates. The presence of a discrete shoulder around $\lambda = 508$ nm followed by a long tail (Fig. 10) let us suspect that the formation of J-aggregates traces also occur for this dye. Nevertheless, J-aggregates usually give narrow bands with small Stokes shifts compared to the absorption band of the dye in the non-associated state; thus, physical aggregation could be responsible of this tail.

The absorption spectrum of **RED-H** shows $\lambda_{max} = 500$ nm (36 nm red-shifted compared to methanol solution) preceded by a band in the blue region at $\lambda = 402$ nm, due to H-aggregates. There is no evidence of the presence of J-aggregates for this dye in film. Absorption bands of **RED-H** exhibit higher red-shifts in the cast film (compared to methanol solution) than those observed for **RED-PEGM** dyes. This can be due to the difference in CT character between the dyes, which agrees with dipole moment values estimated by DFT calculations. Since RED-H has no bulky substituents, usual H-type aggregation occurs generating parallel dimmers, as has also been observed for **RED-PEGM-3**. However, although J-aggregation does occur for **RED-PEGM-3** no J-aggregates were observed for **RED-H** (Fig. 10). We speculate that the short PEGM chain could be able to coil around the nitro group of a neighboring molecule, thus, stabilizing the J-aggregates. Unlike **RED-PEGM-3**, the bulkiness of the PEGM segment in **RED-PEGM-8** inhibits the formation of parallel "face to face" H-aggregates [12]. Rather,

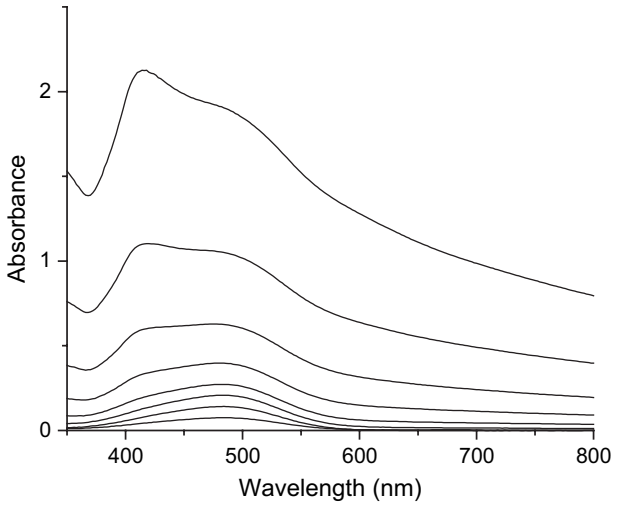

Fig. 9. UV–vis spectra of **RED-H** in methanol:water 20:80. (a) 0.0005 M, (b) 2.5×10^{-4} M, (c) 1.87×10^{-4} M, (d) 1.25×10^{-4} M, (e) 7.5×10^{-5} M, (f) 3.75×10^{-5} M, (g) 1.82×10^{-5} M, (h) 0.93×10^{-5} M, (i) 0.46×10^{-5} M.

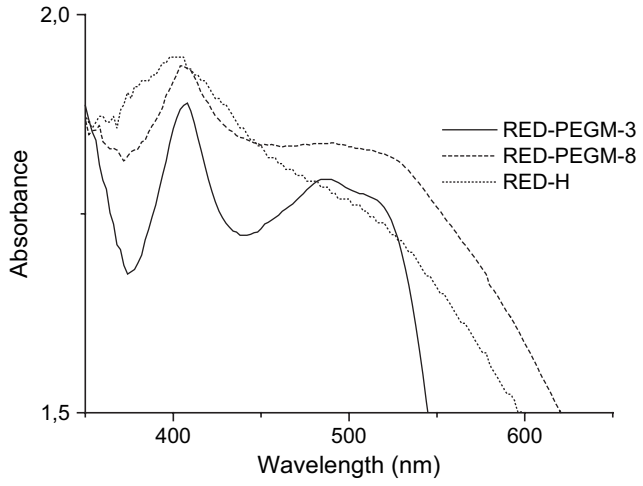

Fig. 10. UV–vis spectra of **RED-PEGM-3**, **RED-PEGM-8**, and **RED-H** in casted film (from $CHCl_3$ solution).

solid state **RED-PEGM-8** molecules form antiparallel H-aggregates to avoid steric interactions as was the case in solution. Similar observations have also been reported by Natansohn et al., using an analogous azobenzene mesogen tethered to a polymethacrylate backbone (p4MAN, $\lambda_{max} = 402$ nm) [17].

3.3. Aggregation of the *RED-PEGM* dyes in Langmuir–Blodgett films

Absorption spectra of **RED-PEGM-3** and **RED-PEGM-8** in Y-type LB films are shown in Fig. 11 as a function of the number of layers. **RED-PEGM-3** (Fig. 11A) exhibited $\lambda_{max} = 473$ nm after 10 layers (5 nm blue-shifted compared to methanol solution) due to the presence of weak intralayer H-aggregates. However, increasing the number of layers gradually shifted the λ_{max} to longer wavelengths, reaching 486 nm after 40 layers (8 nm red-shifted compared to methanol solution). This shift shows evidence of the formation of interlayer J-aggregates after a considerable number of layers. In cast films, the absorption spectrum of **RED-PEGM-3** shows a band at $\lambda = 500$ nm which can be attributed to head to tail J-aggregates. This band is red-shifted by 14 nm compared to that observed in Y-type LB films after 40 layers. This can be explained by the formation of atypical head to head J-aggregates in Y-type LB films; this arrangement is imposed by the LB assembly technique.

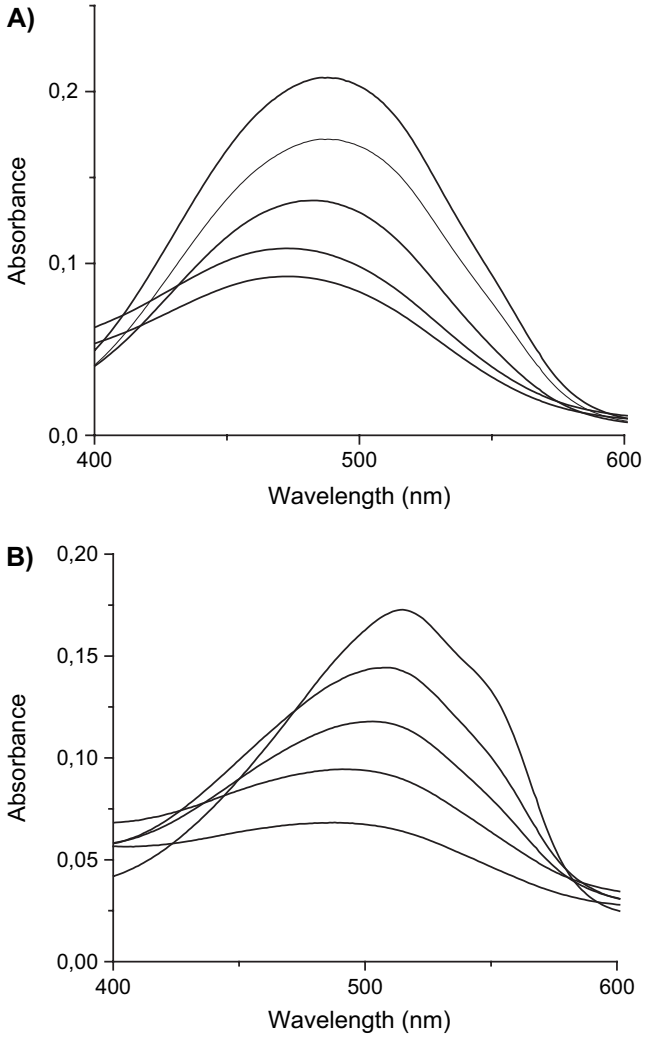

Fig. 11. UV–vis spectra of the LB films of (A) **RED-PEGM-3** (from bottom to top: 5, 10, 20, 30, and 40 layers) and (B) **RED-PEGM-8** (from bottom to top: 2, 10, 20, 30, and 40 layers).

By contrast LB films of **RED-PEGM-8** (Fig. 11B) exhibit a maximum absorption wavelength at 490 nm after 10 layers (red-shifted by 10 nm compared to methanol solution) due to the formation of head to head J-aggregates. The bulky PEGM segment prevents intralayer H-aggregation. After 40 layers, λ_{max} is shifted to 515 nm and the presence of a shoulder at about 540 nm reveals the existence of a second species. This shoulder probably arises from lower energy J-aggregates with longer separation between the azobenzene molecules.

4. Conclusion

All azobenzene dyes form typical parallel H-aggregates in concentrated high water content solutions and in the film. **RED-PEGM-3** is also able to form head to tail J-aggregates in cast films. In Y-type LB films, both **RED-PEGM-3** and **RED-PEGM-8** give rise to head to head J-aggregates. ^{1}H NMR and 2D NOESY experiments revealed that **RED-PEGM-8** forms antiparallel H-aggregates in aqueous solution, jointly with the formation of intramolecular CT complexes by the coiling of the PEGM chain around the azobenzene unit.

Acknowledgements

We thank Miguel Angel Canseco for his assistance with absorption spectroscopy and Dr. Serguei Fomine for his help with DFT calculations. This work was financially supported by DGAPA-UNAM (PAPIIT IN112203-3).

References

[1] Rau H. In: Rabek JK, editor. Photochemistry and photophysics, vol. 2. Boca Raton, FL: CRC Press; 1990. p. 119.
[2] Natansohn A, Rochon P. Can J Chem 2001;79:1093–100.
[3] Todorov T, Nikalova L, Tomova N. Appl Opt 1984;23:4309.
[4] Xie S, Natansohn A, Rochon P. Chem Mater 1993;5:403–11.
[5] Viswanathan NK, Kim DY, Bian S, Williams J, Liu W, Li L, et al. Mater Chem 1999;9:1941.
[6] Ichimura K. Chem Rev 2000;100:1847–74.
[7] Delaire JA, Nakatani K. Chem Rev 2000;100:1817–46.
[8] Natansohn A, Rochon P. Chem Rev 2002;102:4139–75.
[9] Ho MS, Natansohn A, Rochon P. Can J Chem 1995;73:1773.

[10] Meng X, Natansohn A, Rochon P, Barrett C. Macromolecules 1996;29:946–52.
[11] Natansohn A, Xie S, Rochon P. Macromolecules 1992;25: 5531–7.
[12] Kasha M. Rad Res 1963;20:55–71.
[13] Dhanabalan A, Dos Santos Jr DS, Mendonça CR, Misoguti L, Balogh DT, Giacometti JA, et al. Langmuir 1999;15:4560–4.
[14] Dos Santos Jr DS, Mendonça CR, Balogh DT, Dhanabalan A, Giacometti JA, Zilio SC, et al. Polymer 2002;43:4385–90.
[15] Dos Santos Jr DS, Mendonça CR, Balogh DT, Dhanabalan A, Giacometti JA, Zilio SC, et al. Synth Metals 2001;121:1479–80.
[16] Freiberg S, Lagugné-Labarthet F, Rochon P, Natansohn A. Macromolecules 2003;36:2680–8.
[17] Iftime G, Lagugné-Labarthet F, Natansohn A, Rochon P. J Am Chem Soc 2000;122:12646–50.
[18] Lagugné-Labarthet F, Freiberg S, Pellerin C, Pézolet M, Natansohn A, Rochon P. Macromolecules 2000;33:6815–23.
[19] Rivera E, Belletête M, Natansohn A, Durocher G. Can J Chem 2003;81:1076–82.
[20] Dewar MJW, Dieter K. J Am Chem Soc 1986;108:8075–86.
[21] Shin DM, Schanze KS, Whitten DG. J Am Chem Soc 1989;111:8494–501.